Yttrium Nanoparticle Hydrogen Gas Sensors

ARTICLE *in* NATO SECURITY THROUGH SCIENCE SERIES B: PHYSICS AND BIOPHYSICS · JANUARY 2011

DOI: 10.1007/978-94-007-0903-4_39

3 AUTHORS, INCLUDING:

Andrey L. Stepanov

Russian Academy of Sciences

243 PUBLICATIONS **2,596** CITATIONS

Nanotechnological Basis for Advanced Sensors

edited by

Johann Peter Reithmaier
Institute of Nanostructure Technologies and Analytics
University of Kassel
Kassel, Germany

Perica Paunović
University "Sts. Cyril and Methodius"
Skopje, FYR Macedonia

Wilhelm Kulisch
Department of Mathematics and Natural Sciences
University of Kassel
Kassel, Germany

Cyril Popov
Institute of Nanostructure Technologies and Analytics
University of Kassel
Kassel, Germany

and

Plamen Petkov
Department of Physics
University of Chemical Technology and Metallurgy
Sofia, Bulgaria

Published in Cooperation with NATO Emerging Security Challenges Division

Chapter 39
Yttrium Nanoparticle Hydrogen Gas Sensors

Andrey L. Stepanov, Alexander Reinhodt, and Uwe Kreibig

Abstract The preparation of new types of nanosystems based on metallic yttrium nanoparticles, which are difficult to produce by traditional methods due to the high melting temperature and the extremely high oxidizability of this metal, has been studied. The materials were prepared with an original high vacuum set-up (LUCAS) intended for the formation of metal nanoparticle beams by laser ablation. Yttrium nanoparticles were synthesized, and their chemical reactions with hydrogen were studied at room temperature. It was found that the reaction at low hydrogen pressures (~10^{-3} Pa) leads to the formation of YH_2 dihydride particles with metallic properties and optical plasmon absorption. An increase in the hydrogen pressure to ~100 Pa results in the transformation of metallic-like YH_2 nanoparticles to dielectric YH_{3-x} ($x < 1$) nanoparticles. It is shown that the last reaction corresponding to the metal–dielectric phase transition is reversible with respect to the hydrogen pressure. These experimental data demonstrate that yttrium nanoparticle materials can be effectively used as optical hydrogen gas sensors.

Keywords Hydrogen gas sensor · Yttrium-based nanoparticles · Yttrium dihydride · Laser ablation · Plasmon resonances

Introduction

At present, nanostructured materials, in particular metal nanoparticles (MNPs) or clusters, have been extensively investigated from fundamental and applied viewpoints. MNPs occupy an intermediate position between molecular species and bulk

A.L. Stepanov (✉)
Kazan Physical-Technical Institute, Russian Academy of Sciences,
Sibirsky trakt 10/7, 420029 Kazan, Russia;
Kazan State University, Kremlevskaya 18, 420008 Kazan, Russia;
and
Laser Zentrum Hannover, Hollerithallee 8, 30419 Hannover, Germany
e-mail: aanstep@gmail.com

A. Reinhodt and U. Kreibig
I. Physikalisches Institut der RWTH, Sommerfeldstrasse 8, 52056 Aachen, Germany

J.P. Reithmaier et al. (eds.), *Nanotechnological Basis for Advanced Sensors*,
NATO Science for Peace and Security Series B: Physics and Biophysics,
DOI 10.1007/978-94-007-0903-4_39,

materials and exhibit new properties that arise either as a result of the small number of atoms in a particle ("size effect") or due to the strong influence of the interface between MNPs and the environment ("surface effect") [1]. The present work is devoted to the preparation of a new nanostructured material based on transition metal (yttrium) nanoparticles and, the study of surface effects in these MNP systems. It should be noted that metallic yttrium nanoparticles are quite difficult to synthesize by conventional physical methods, such as vacuum deposition, sol–gel synthesis, and other techniques, due to the high melting (1,522°C) and boiling (2,927°C) temperatures of yttrium, as well as the extremely high oxidizability. Moreover, as was shown in Refs. [2–5], bulk samples of metallic yttrium are characterized by a high chemical reactivity with respect to hydrogen. These physicochemical features of yttrium gave impetus to investigations of the synthesis of yttrium nanoparticles and the influence of hydrogenation of the nanoparticles on their optical and electrical properties.

Experimental Procedure

The high vacuum laser-based universal cluster ablation source (LUCAS) was designed for synthesizing yttrium nanoparticles with a high chemical reactivity [6]. Nanoparticles were produced using a LUMONICS JK 702H pulsed Nd:YAG laser operating at a wavelength of 1.064 μm. A beam of yttrium particles was generated by laser ablation of chemically pure metallic bulk yttrium in argon atmosphere at pressures of 6.0–1.2 Pa. The plasma generated by the laser pulses above the surface of the yttrium target was cooled by atoms of the inert gas fed in the chamber. The gas mixture of argon and yttrium particles was ejected from a nozzle with a diameter of 1.2 mm due to the pressure difference between source and deposition chamber produced by vacuum pumps. The pressure in the deposition chamber was approximately equal to 6.0×10^{-4}–1.2×10^{-5} Pa. The laser ablations was performed using 500 pulses with an energy density of ~4.7 J/cm^2, a pulse duration of 1 ms, and a frequency of 80 Hz. The MNPs were deposited onto quartz substrates or carbon thin films intended for electron microscopic analyses, which were carried out with a Philips EM 400T transmission electron microscope.

After deposition, the samples with the yttrium nanoparticles were exposed from 30 min to several hours to hydrogen atmospheres at pressures in the range from 5×10^{-4} to 500 Pa at room temperature. In order to provide in-situ chemical reactions between hydrogen and yttrium nanoparticles, the MNPs were coated in a vacuum chamber by a palladium thin film (~0.3 mm) by electron beam evaporation. The palladium served for the formation of a hydrogen solution, which favored the incorporation of hydrogen into the yttrium particles. The phase composition of the nanoparticles was controlled by measuring in-situ the optical extinction spectra with a single beam fiber-optic set-up based on a Zeiss MSC spectrometer in the range 250–1,000 nm. The electrical resistance of the samples containing

hydrogenated yttrium nanoparticles was in-situ measured according to the standard procedure by the four point probe method using a Keithley 236 source unit, which made it possible to measure currents from fA to nA. The voltage between the contacts was equal to 1 V, the distance between the gold contacts 4.5 mm.

Fabrication of Yttrium Nanoparticles

Electron micrographs of yttrium nanoparticles with two scales and the corresponding histograms of their size distributions are shown in Fig. 39.1 for different argon pressures. It can be seen that the nanoparticles are almost spherical. Data on the average size d of the nanoparticles and the standard deviation σ from the average are also presented in figure. It was revealed that larger nanoparticles with a narrower size distribution are formed at the higher argon pressure (1.2×10^5 Pa). The average sizes of yttrium nanoparticles synthesized at pressures of 6.0×10^4 and 1.2×10^5 Pa are 25 and 30 nm, respectively. The observed dependence of the size of yttrium nanoparticles on the gas pressure is qualitatively in agreement with the results of investigations of the formation of semiconductor particles [7] and silver and copper nanoparticles [8] formed by laser ablation. However, in our case, the value of σ obtained at a pressure of 1.2×10^5 Pa appears to be considerably lower than those determined in [7,8]. An interesting feature, which was observed in the case of yttrium nanoparticles but not in earlier experiments, is that the surface of the nanoparticles is covered by a shell (Fig. 39.1b). It was established that this shell appears on the MNPs at argon pressures above 6×10^4 Pa and that the shell thickness increases with increasing pressure. A high resolution electron micrograph of yttrium nanoparticles with shells of varying thickness is displayed in Fig. 39.2. It can be seen from this figure that the shell thickness can be as large as ~4–6 nm. It should also be noted that, since the shell between yttrium particles in direct contact is absent, the inference can be made that the shell is formed within a certain time after the formation of the MNPs. Since the shell appears for nanoparticles synthesized at high pressures of the seeding gas, we can assume that the MNPs undergo surface oxidation due to the presence of residual oxygen in the gas phase.

In this case, we can expect the formation of a dielectric phase Y_2O_3, which is known easily form on the surface of metallic yttrium films in air [6]. To check this assumption, we performed in situ measurements of the absorption (optical density) of yttrium nanoparticles without and with shells, which were prepared at low and high argon pressures, respectively. Figure 39.3 shows the experimental optical density spectra of the nanoparticles. The absorption spectrum of yttrium particles exhibits the well-known band with a maximum in the range of ~380 nm due to the surface plasmon resonance in MNPs [1,9]. Unlike yttrium nanoparticles, the absorption spectrum of particles with shells is characterized by a considerably broader band that covers almost the entire visible range with the maximum shifted toward longer wavelengths to approximately 650 nm. Moreover, an enhancement

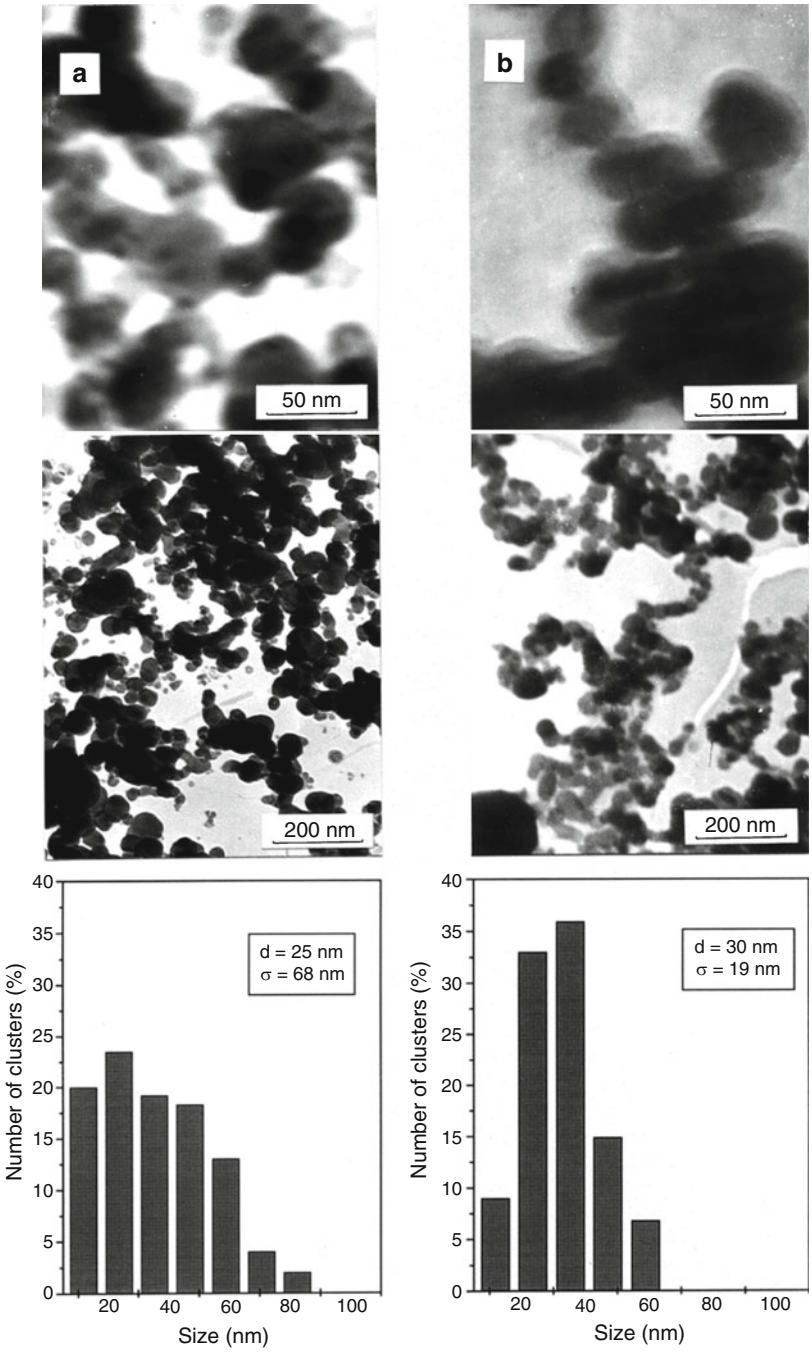

Fig. 39.1 Electron micrographs and histograms of the size distributions of yttrium nanoparticles synthesized at argon pressures of (**a**) 6.0×10^4 and (**b**) 1.2×10^5 Pa

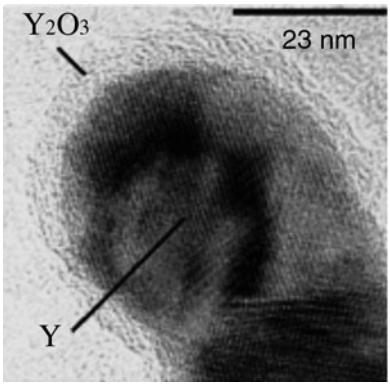

Fig. 39.2 High resolution electron micrograph of yttrium nanoparticles with shells of different thickness

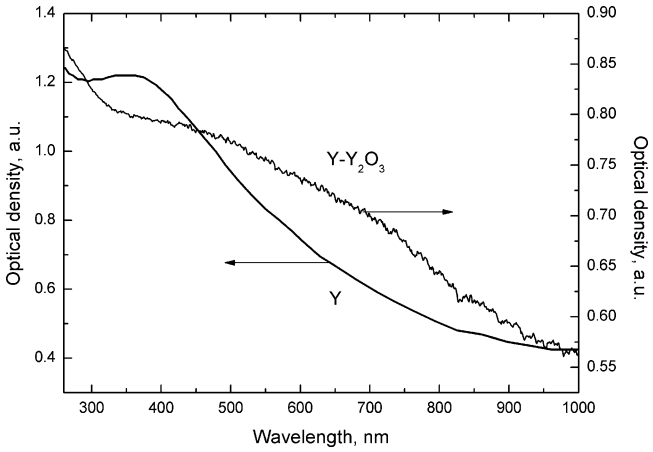

Fig. 39.3 Experimental optical density spectra of yttrium nanoparticles without and with shells, synthesized at argon pressures of 6.0×10^4 and 1.2×10^5 Pa, respectively

of the absorption in the UV spectral range below 300 nm is observed in the spectrum. In order to explain these experimental results, the extinction spectra of complex particles consisting of an yttrium core and an yttrium oxide shell were simulated using the electromagnetic theory of Mie [10,11]. In our calculations, the thickness of the Y_2O_3 shell varied from 0 to 20 nm, whereas the core size remained constant (30 nm). The permittivities of Y and Y_2O_3 required for the calculations were taken from Ref. [12].

The calculated spectra are shown in Fig. 39.4. It can be seen from this figure that the presence of Y_2O_3 shells on the surface of yttrium nanoparticles leads to a shift in the extinction maximum toward the red spectral range and, in addition, to an increase of the absorption in the UV range. Although the experimental and simulated spectra are only in qualitative agreement (this can be associated with

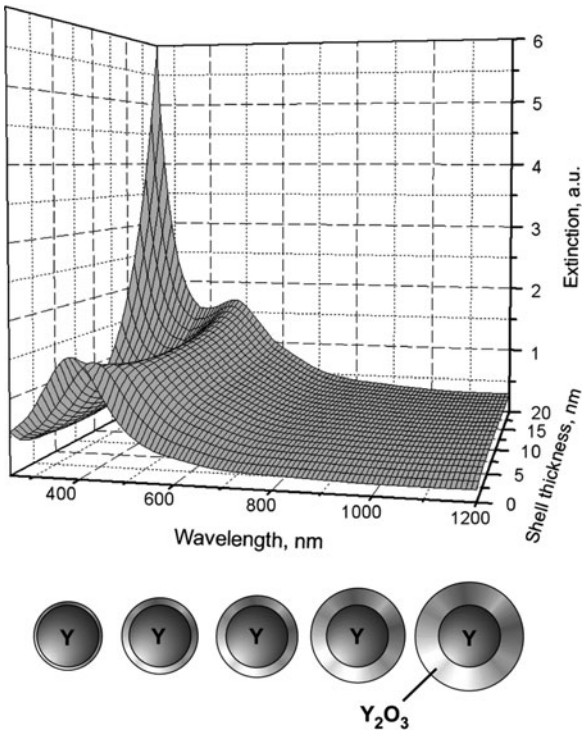

Fig. 39.4 Calculated optical extinction spectra of yttrium nanoparticles with Y_2O_3 shells as a function of the shell thickness

difficulties encountered in calculating the particle size distribution and the variable thickness of the shells), we should note two coinciding spectral features: the shift of the maximum to longer wavelengths and the increase in the absorption intensity in the UV range in the presence of oxide shells. This circumstance gives ground to suggest that the surface shells observed for yttrium particles in the micrographs (Figs. 39.1and 39.2) are caused by the oxidation of the MNPs.

Fabrication of Hydrogenated Yttrium Nanoparticles

Since, as was shown in the previous section, yttrium nanoparticles are prone to oxidation, we chose samples synthesized at a low argon pressure (6×10^4 Pa) for hydrogen experiments. The average size of the nanoparticles in these samples remained almost unchanged after the chemical reaction with hydrogen. Previously, in experiments on hydrogenation of bulk yttrium thick films, the types of crystal structures corresponding to the yttrium phase and the newly formed yttrium hydride phases were determined using X-ray diffraction [5]. Furthermore, for the same hydrogenated yttrium films, these authors determined the dielectric constants of [5]

which were subsequently used in [13] to calculate the optical extinction spectra of nanoparticles of different phase compositions Y and YH_{3-x} (from $x < 1$ to $x << 1$) in the framework of the Mie theory. In this respect, the available calculated spectra can be used for determining the phase composition of the hydrogenated nanoparticles produced in our work.

In order to hydrogenate yttrium nanoparticles, the samples were coated by a thin continuous palladium film in which a hydrogen solution was formed. It was revealed that the presence of the palladium film does not substantially affect the initial optical spectra of the yttrium nanoparticles. Exposure of the yttrium nanoparticles to different hydrogen pressures results in a significant change in their optical extinction spectra (Fig. 39.5). Exposure of yttrium to low hydrogen pressures (~10^{-3} Pa) leads to the formation of particles of a new yttrium dihydride (YH_2) phase with a face-centered cubic lattice due to the occupation of face-centered cubic interstitial positions in the hexagonal close-packed yttrium lattice by hydrogen atoms [4]. According to earlier calculations [13], only in the case of small particles (Fig. 39.6, hydrogen pressure 5.0×10^{-4} Pa) the YH_2 phase is characterized by two spectrally resolved bands of optical Mie resonances (400 and 960 nm), which are considerably narrower than those for yttrium nanoparticles. The YH_2 particles also exhibit metallic properties and have a stable structure. Since a decrease of the hydrogen pressure (complete evacuation of hydrogen from the chamber) does not result in any change in the optical spectrum of the YH_2 nanoparticles, we can assume that their phase composition is retained. As for the bulk materials [5], in the case of the nanoparticles the chemical reaction $Y \Leftrightarrow YH_2$

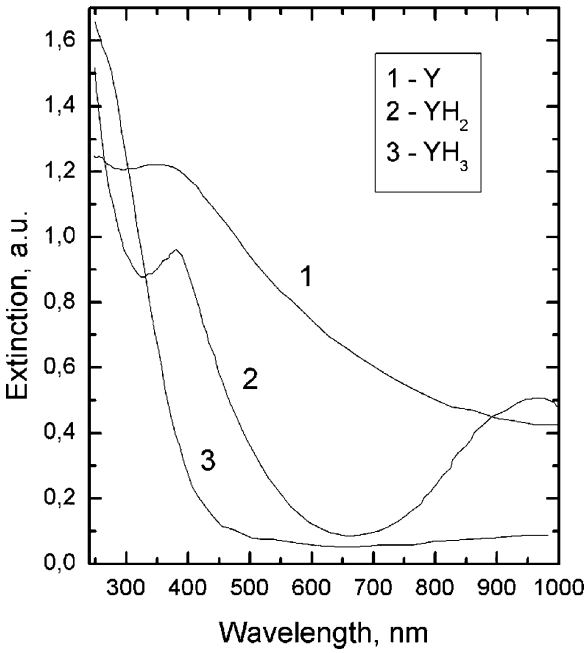

Fig. 39.5 Experimental optical extinction spectra measured in situ for (*1*) Y, (*2*) YH_2, and (*3*) YH_3 nanoparticles

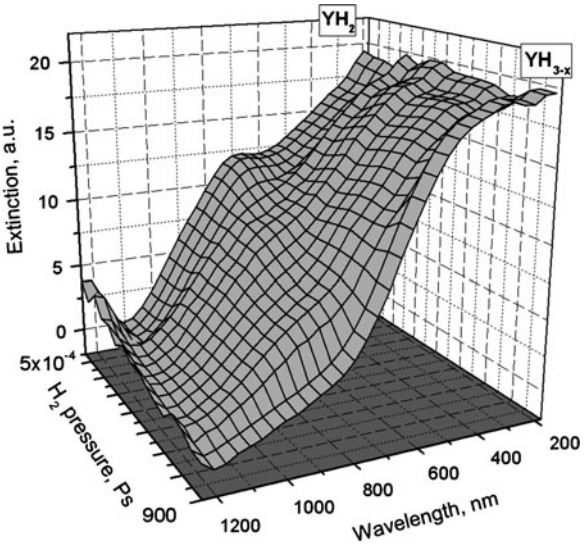

Fig. 39.6 Experimental optical extinction spectra measured in situ and illustrating the reaction YH2 ⇔ YH3 at different hydrogen pressures

is irreversible. The optical reflection from deposited YH_2 particles is characterized by a metallic surface, as is the case of yttrium nanoparticles.

Figure 39.6 shows a series of extinction spectra measured in situ for samples in hydrogen atmosphere as a function of the hydrogen pressure. The spectrum of yttrium nanoparticles is not shown in this figure. As can be seen from Figs. 39.5, 39.6, a gradual increase of the hydrogen pressure leads to a monotonic change in the optical spectra, which manifests itself in a smooth decrease of the intensity of the selective extinction bands down to their complete disappearance. By analogy with a study of bulk yttrium films [4], we can suggest that an increase in the hydrogen pressure (in our experiment to a level of ~100 Pa) results in a change in the phase composition with the formation of nanoparticles of yttrium trihydride YH_{3-x} (from $x < 1$ to $x \ll 1$) due to the incorporation of hydrogen atoms on interstitial positions the hexagonal close-packed crystal lattice of the YH_2 phase. In this case, the metallic luster of the YH_2 nanoparticles disappears. Curve 3 in Fig. 39.5 and the curve corresponding to a hydrogen pressure of 900 Pa in Fig. 39.6 characterize the $YH_{\sim 3}$ nanoparticles, which have a hexagonal close-packed structure. The optical density spectrum of these particles is typical of small dielectric particles [1]: the absence of selective absorption bands in the visible range and a monotonic increase of the absorption in the UV range. The chemical reaction $YH_2 \Leftrightarrow YH_3$ turns out to be reversible at room temperature with respect to the hydrogen gas pressure. This effect manifests itself as a reversible change in the optical spectra upon sequential multiple (no less than ten times) increase and decrease of the hydrogen pressure in the deposition chamber of the set-up, which is also confirmed by reversible changes in the electrical conductivity. Such a change in the phase composition of hydrogenated yttrium particles seems to be promising from the

standpoint of the design of optical or electrical hydrogen gas sensors and detectors, because the observed phase transition is accompanied by a substantial change in both the optical spectrum (from absorbing to transparent in the visible range) and the conductivity of the sample. Composite materials based on these nanoparticles possess a number of obvious advantages over, for example, thick brittle yttrium films [5]. The first is the more developed surface of small particles, which increases the efficiency of the interaction with hydrogen. Second, the nanoparticles are less prone to mechanical stresses and damage that arise because the transition $YH_2 \Leftrightarrow YH_3$ is accompanied by a change in the lattice constant by up to 10%.

Acknowledgements The author is grateful to the Alexander von Humboldt Foundation (Germany) and the Austrian Scientific Foundation in the frame of the Lise Meitner program for financial support. This work was partly supported by the Russian State Contract No. 02.740.11.0797.

References

1. U. Kreibig and M. Vollmer, Optical properties of metal clusters, Springer, Berlin (1995).
2. H.E. Flotow, D.W. Osborne, K. Otto, and B.M. Abraham, J. Chem. Phys. **38**, 2620 (1963).
3. L.N. Yannopoulos, R.K. Edwards, and P.G. Wahlbeck, J. Chem. Phys. **69**, 2510 (1965).
4. J.N. Huiberts, R. Griessen, J.H. Rector, R.J. Wijngaarden, J.P. Dekker, D.G. de Groot, and N.J. Koeman, Nature **380**, 231 (1996).
5. J.N. Huiberts, J.H. Rector, R.J. Wijngaarden, S. Jetten, D. de Groot, B. Dam, N.J. Koeman, R. Griessen, B. Hjörvarsson, S. Olafsson, and Y.S. Cho, J. Alloys Comp. **239**, 158 (1996).
6. A.L. Stepanov, M. Gartz, G. Bour, A. Reinholdt, and U. Kreibig, Vacuum **67**, 223 (2002).
7. W. Marine, L. Patrone, B. Luk'yanchuk, and M. Sentis, Appl. Surf. Sci. **154-155**, 345 (2000).
8. Z. Pászti, Z.E. Horváth, G. Petõ, A. Karacs, L. Guczi, Appl. Surf. Sci. **109-110**, 67 (1997).
9. M. Gartz, and M. Quinten, Appl. Phys. B **73**, 327 (2001).
10. G. Mie, Ann. Phys. **25**, 377 (1908).
11. A.L. Stepanov, in: Metal-Polymer Nanocomposites, L. Nikolais and G. Carotenuto (Eds.), Wiley, Danvers (2004).
12. E.D. Palik, Handbook of optical constants of solids, Academic Press, London (1997).
13. G. Bour, A. Reinholdt, A.L. Stepanov, C. Keutgen, and U. Kreibig, Eur. Phys. J. D **16**, 219 (2001).